Utilizing Faujasite-type zeolites prepared from waste aluminum foil for competitive ion-exchange to remove heavy metals from simulated wastewater

Sama M. Al-Jubouri[a,*], Sirhan I. Al-Batty[b], Sivasakthi Senthilnathan[c], Norrapat Sihanonth[c], Lal Sanglura[c,d], Hongjin Shan[c], Stuart M. Holmes[c]

[a]*Department of Chemical Engineering, College of Engineering, University of Baghdad, Aljadria, Baghdad, Post code: 10071, Iraq,*
email: sama.al-jubouri@coeng.uobaghdad.edu.iq
[b]*Department of Chemical and Process Engineering Technology, Jubail Industrial College, Kingdom of Saudi Arabia,*
email: batty_sa@jic.edu.sa
[c]*Department of Chemical Engineering and Analytical Science, The University of Manchester, Manchester M13 9PL, UK,*
emails: smileysakthi@hotmail.com (S. Senthilnathan), norrapat44@gmail.com (N. Sihanonth), ersanglurack13@gmail.com (L. Sanglura),
791846842@qq.com (H. Shan), stuart.holmes@manchester.ac.uk (S.M. Holmes)
[d]*Mizoram Civil Service, Government of Mizoram, Mizoram, India*

ABSTRACT

The pollution by heavy metal ions is a severe risk for aquatic and earthy living creatures. Ion-exchange is an easy way to eliminate heavy metal pollution. Different ion-exchangers have been developed and applied for wastewater and other environmental treatments, such as zeolites. The synthesis of zeolites from inexpensive sources is very important in the minerals industry. The recycling of the waste aluminum foil to obtain the alumina source for the preparation of NaY zeolite and NaX zeolite was investigated in this study. Both Faujasite-type zeolites were obtained by a conventional hydrothermal treatment of the gel at 100°C for 24 h. The prepared zeolites were characterized by X-ray diffraction (XRD), scanning electron microscopy (SEM), energy dispersive analysis by X-ray (EDAX), and nitrogen adsorption/desorption isotherms. The synthesized NaY zeolite and NaX zeolite based on aluminum foil had a Si/Al ratio of 2.28 and 1.35, and a specific surface area of 476.248 and 610.256 m^2/g, respectively. Also, the treatment of the individual, binary, and ternary metals solutions containing Cd(II), Cu(II) and Hg(II) ions was carried out using ion-exchange by NaY zeolite and NaX zeolite. The affinity of both zeolites to the selected metal ions was in the following order: Cd(II) > Cu(II) > Hg(II). The ion-exchange results highly adapted to the pseudo-second-order kinetic model with high correlation coefficients ($R^2 > 0.96$). Furthermore, stabilization of the removed ions inside the spent zeolites was conducted by geopolymers prepared from ordinary Portland cement and fly ash as cement material. Fly ash showed high potential as a solidifying material for the samples examined in the leaching test by H$_2$SO$_4$ solution. The ratio of 1 cement:3 fly ash gave the least leached metals concentration at all testing conditions.

Keywords: Zeolite; Waste aluminum foil; Competitive ion-exchange; Heavy metals; Kinetics

1. Introduction

The rapid development of industries leads to diverse environmental issues including the discharge of large amounts of highly polluted wastewater [1,2]. These polluted waters cause negative impacts on the environment when they are discharged without appropriate treatment. Direct disposal of polluted waters containing heavy metals like cadmium, mercury, lead, copper, chromium, cobalt, zinc, and strontium, etc., is one of the major causes of pollution [3,4]. These heavy metals generally present in wastewaters

---

* Corresponding author.

released from mining, electroplating, metal processing, textile, battery manufacturing, tanneries, petroleum refining, paint manufacture, pesticides, fertilizers, pigment manufacture, printing, and photographic industries [5,6]. The concerns of heavy metals increased due to the difficulty of the elimination process from industrial wastewaters containing different types of heavy metal ions and organic pollutants. Besides, heavy metals cause severe problems for the environment and influence public health [7–9].

Cadmium (Cd(II)) is one of the most poisonous metals even more toxic than mercury. Even at low concentrations levels, it leads to disorders such as brain damage, bone diseases, pulmonary edema, trachea-bronchitis, lung cancer, skin cancer, anemia, kidney damage, diabetes, and heart diseases [10,11]. Likewise, mercury (Hg(II)) deemed as an extremely toxic metal that is widely present in the soil, water, and air. Its toxicity causes kidney injury, chronic diseases, respiratory failure, central nervous system disorders, brain damage, and severe environmental pollution even at low concentration levels. Moreover, Hg(II) can pass into the food chain because it possesses a non-biodegradable property. Other heavy metals such as copper (Cu(II)) leads to irritation of the nose, eyes, mouth, headache, and stomachache when exposed for a long time [12–14].

Different techniques have been mentioned in the literature [14–17] that can be used to eliminate heavy metals such as chemical precipitation, coagulation/flocculation, ion-exchange, solvent extraction, electro-chemical operations, biological operations, adsorption, evaporation, filtration, and membrane processes. The most significant drawback of using these techniques is the cost, such as electrochemical operations, evaporation, and membrane processes. Moreover, some of them require additional chemicals in order to achieve the removal process such as chemical precipitation, coagulation/flocculation, and solvent extraction. But in these methods, subsequent treatment is required to remove the used chemicals [18,19]. Meanwhile, other methods are highly effective in the presence of a high concentration of pollutants, such as filtration, and chemical precipitation. Biological operations require special attention in terms of avoiding the spoiling of the digesting biomass [20]. Most of these defects can be overcome when using inexpensive, abundant, efficient ion-exchangers or adsorbents having a high affinity for heavy metals. Ion-exchange can treat low-medium pollutant concentrations at normal conditions and simple equipment with a potential possibility of regeneration or safe disposal [21].

Adsorption is one of the most promising techniques, especially when using cheap-abundant and effective organic and inorganic adsorbents [22]. Inorganic adsorbents such as zeolites, titanate-based materials, carbon-based materials, and minerals have high stability in high radiation environments and found more appropriate for radioactive waste removal when compared with organic adsorbents [23]. Interestingly, the adsorption process allows cost-effective simple treatment of pollutants using the same materials that are used in other sophisticated treatment technologies. For example, a research group [24] fabricated a kind of MWCNTs-based nanocomposite as an adsorbent for the removal of Pb(II) from an aqueous solution, which was used as a catalyst in the photocatalytic reduction for Cr(VI) removal [25]. In the same way, another group [26] replaced electrochemical determination with a simple adsorption process using kinds of zirconium dioxide composite for the treatment of pollutants [27].

Ion-exchange is a widely spread technique used to treat aqueous streams polluted with different metal ions because of its efficiency, selectivity, and easiness [28]. The ion-exchange materials are available in various forms and structures based on morphology (physical form), origin, fixed functional group, and their functions. Therefore, the ion-exchange mechanism is commanded by different parameters associated with the ion-exchange materials, including the type and nature of immobilized functional groups, the origin, and the morphology of the ion-exchange material. There are two main types of ion-exchange materials. The first type is organic which are exists in anionic and cationic forms of synthetic polymers, such as chelating resins, zwitterionic polymers, retardion 11-A-8 resin, amberlite IRA 743 resin, Dowex XUS 43594 resin, Purolite S 108 resin, and Diaion WA 30 resin. The second type is minerallic (inorganic) ion-exchangers which are available in cationic form only, such as zeolites and bentonite [29]. Inorganic ion-exchange materials have been increasingly replaced or complemented for conventional organic ion-exchange resins, especially for treating radioactive waste. This is because inorganic ion-exchangers have high selectivity and radiation stability for specific radiological species, like strontium and cesium [28]. Therefore, zeolites are suitable cationic ion-exchangers for the removal of heavy metal ions [29]. Zeolites are commonly excellent ion-exchangers that can immediately exchange the positively-charged metal cations via easily exchangeable cations present in their structure [20].

Zeolites are microporous aluminosilicates having a negative-charged surface because of the presence of Al in their framework [30,31]. Zeolites are different types and have a wide range of applications such as ion-exchange, catalysis, softening, optics, medical and pharmaceutical applications, and photochemistry due to their outstanding ion-exchange properties, shape-selectivity, and higher surface area [32,33]. Since the structure of zeolites consists of alumina and silica tetrahedrons [34], they can be prepared from different raw materials providing Si, Al with the consideration of cost and pure final product [35]. Some researchers have focused on recycling different types of waste such as rice husk [36], aluminum scraps [37], barley husk [38], coal fly ash [39], and Phragmites (common water reeds) [40,41]. Recycling large amounts of waste containing aluminum by transforming it into useful materials has a positive impact on human health such as the nervous system and the environment. This is because its presence hinders the growth of plant roots by influencing the adsorption of nutrients and water [37]. X and Y zeolite belong to the Faujasite family which has a high cation availability for exchange. However, X zeolite demonstrates better ion-exchange performance than Y zeolite due to its low Si/Al ratio [42,43].

Using an ion-exchange method to remove heavy metals via zeolites requires an additional step to treat the spent zeolites. Solidification/Stabilization (S/S) technology has been used for treating banned waste before landfilling and found effective for the immobilization of heavy metal contaminants [44]. To treat hazardous materials, special

landfill areas equipped with leaching collecting systems are required. The S/S technology can prevent the exposure of the environment to hazardous contaminants by encapsulating these contaminants to ensure safe landfilling based on the high mechanical properties of the used materials. The low operational cost of S/S is due to the use of cheap materials such as cement and limes which make the process simpler and feasible [45]. Geopolymers have been introduced to S/S as binders such as those used in concrete [46]. Fly ash is a by-product of combustion activity that has low cost and highly abundant. Fly ash can be used in S/S to reduce the cost of S/S and enhance the fixation of contaminants [47].

This study focuses on converting aluminum foil waste into useful crystalline aluminosilicates for wastewater treatment and the solidification of harmful pollutants. NaY zeolite and NaX zeolite will be prepared using the conventional hydrothermal treatment of the gel-based recycled aluminum foil to obtain a cheap alumina source. Also, this work investigates the removal of Cd(II), Cu(II) and Hg(II) ions from simulated aqueous solutions containing individual, binary and ternary metals using ion-exchange by the synthesized zeolites. The kinetics of the ion-exchange process for the solutions containing binary and ternary metals has been studied using pseudo-first-order model and pseudo-second-order model. Moreover, the solidification of the spent metal-bearing zeolite will be investigated using geopolymers made from Cement/fly ash.

2. Experimental work

2.1. Materials

The waste aluminum foils were collected from various local places and recycled to prepare sodium aluminate as an alumina source. The other materials used for preparing zeolites were: sodium hydroxide (99.9% wt.) provided by Fisher Scientific, LUDOX AS-40 provided by Sigma-Aldrich, and sodium silicate silica ($SiO_2:Na_2O = 2:1$) provided by Fisher scientific were used as silica source. The materials used for ion-exchange experiments were: copper(II) nitrate trihydrate (99% wt.), cadmium(II) nitrate tetrahydrate (98% wt.), and mercury(II) nitrate monohydrate (98% wt.) were all provided by Sigma-Aldrich to obtain metals solutions. Fly ash provided by Cemex 450-S, Portland cement (Procem only) provided by Lafarge, and Portland-Limestone cement provided by Lafarge were used to prepare geopolymers. Sodium chloride (99.5% wt.) provided by BDH laboratory and sulfuric acid (96% solution in water) provided by ACROS Organics for metal ions leaching study.

2.2. Recycling aluminum foil to obtain alumina source

To prepare the sodium aluminates solution from waste material, the collected aluminum foils were first washed with tap water followed by distilled water to remove oil, dirt, and impurities. The washed aluminum foil was then sonicated in acetone media for 10 min, washed with deionized water, dried, and kept ready for use. After that, 100 mL of 10 M NaOH solution was added to a beaker containing the clean aluminum foil. This step was conducted inside a fume cupboard to avoid the risk associated with the exothermic reaction of the sodium aluminates formation as shown in Eq. (1):

$$2Al + 2NaOH + 2H_2O \rightarrow Al_2O_3 + Na_2O + \uparrow 3H_2 \qquad (1)$$
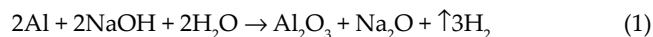
The result of this reaction is a gel-like solution with foam which was separated using filter papers to obtain a clear gel-like solution for zeolite preparation. To assure successful preparation of the target zeolites, the composition of the sodium aluminates solution must be estimated accurately. The composition was obtained by making a mass balance on the resulted batch of the sodium aluminates solution. The results of mass balance led to that sodium aluminates solution contains 17.3% wt. of Al_2O_3 and 10.5% wt. of Na_2O with a density of 1.6 g/mL.

2.3. Synthesis of NaY zeolite and NaX zeolite

The synthesis gel of NaY zeolite was prepared with a molar ratio of $4.63Na_2O:Al_2O_3:9SiO_2:174.2H_2O$ according to the procedures mentioned in the previous work [35] with some modifications. A seeding gel was prepared with a molar formula of $11.21Na_2O:Al_2O_3:9SiO_2:183.4H_2O$. This gel was statically aged at room temperature. Then 4 g of seeding gel (containing 8.5% of Al_2O_3) was added to a feedstock gel prepared with a molar formula of $4.07Na_2O:Al_2O_3:9SiO_2:173.4H_2O$. Mixing time was decently increased for each step to assure obtaining a homogenous gel. The obtained quantity of gel was crystallized at 100°C for 12, 16, 20, and 24 h due to change the alumina source (from waste aluminum foil) to investigate which time gives a better product. After that, the produced zeolite was collected as usual procedures used in the literature [48].

The molar ratio of the synthesis gel used to prepare NaX zeolite was $5.6Na_2O:Al_2O_3:4SiO_2:260H_2O$ which was prepared according to the procedures mentioned in previous work [49]. Also, the mixing time was slightly prolonged due to changing the alumina source and achieving a homogenous gel. The produced gel was crystallized at 100°C for 6, 8, 12, 18, and 24 h after overnight aging and continuous mixing. Also, the produced NaX zeolite samples were collected in the same way used to collect NaY zeolite samples.

2.4. Characterization

A Miniflex Rigaku X-ray analytical instrument was used to obtain XRD patterns of the zeolite samples. The instrument works with a radiation source of CuKα ($\lambda = 1.5418$ Å, voltage = 30 kV, and current = 30 mA) and the analysis was conducted with 2θ ranging = 5°–50°, a step size = 0.03, and a scan speed = 3°min^{-1}. Scanning microscopy model FEI Quanta 200 instrument was used to obtain SEM images of the samples which have to be coated with gold. Also, the same instrument was used to obtain a quantitative analysis using EDAX. ImageJ software was used based on XRD data to obtain the average crystal size of the zeolite samples [50]. Micromeritics ASAP 2020 was used to obtain the specific surface area and pore volume using the

Brunauer–Emmett–Teller (BET method) through measuring the nitrogen adsorption/desorption isotherms at –197°C.

2.5. Ion-exchange experiments

The heavy metal solutions were prepared by dissolving copper nitrate, cadmium nitrate, and mercury nitrate in deionized water. The first set of ion-exchange experiments were conducted for individual ion solution cadmium, copper, and mercury solutions at a fixed initial ion concentration of 200 ppm, mixing speed (Smix) of 200 rpm, room temperature (Troom) but different zeolite doses of 1, 2, 3, 4, and 5 g/L. Two other sets of experiments were conducted as binary metals solution (Cd + Cu, Cd + Hg, and Cu + Hg) and ternary metals solution (Cu + Cd + Hg) at a fixed zeolite dosage of 5 g/L, initial ion concentration of 200 ppm and mixing speed of 200 rpm at room temperature. For all experiments, the pH of the solutions was measured at the beginning and end of the experiment time. Also, liquid samples were collected at different intervals 1, 2, 3, 4, and 24 h; and measured for ions concentration. Inductively coupled plasma-optical emission spectroscopy (ICP-OES) model Vista-MPX was used to obtain the concentrations of the remaining ions in the samples collected during the ion-exchange. The spent zeolites were filtered, dried overnight, and characterized by EDAX.

2.6. Solidification of the spent zeolites

The procedures conducted in this section of the study were inspired by other published works [32,51] with few modifications. This study was carried out using the spent zeolites resulting from the ion-exchange process conducted to remove the combination of Cd, Cu, and Hg ions from aqueous solutions. As these metal ions have different boiling points that are 766.8°C for Cd, 2,562°C for Cu, and 356.7°C for Hg; solidification of the spent zeolites using geopolymers is an appropriate way to avoid sublimating of the metal ions during vitrification. Solidification of the materials used to encapsulate the spent zeolites requires an activation solution that was prepared by mixing 0.5 mL of sodium silicate solution and 2.5 mL of 10 N NaOH solution. The cement/activator solution ratio is an important factor as it decides the strength of the matrix structures through its role in the mixing, freestanding water, and capability for immersion test. Therefore, three different cement:fly ash mixtures were prepared with different weight ratios (3:1, 1:1, and 1:3). These samples were compared with a sample prepared from a Portland-limestone cement containing 25% wt. fly ash. The preparation of the spent zeolite-geopolymer samples started with mixing cement and fly ash with considering the above ratios. After that, 3 g of the geopolymers mixture was mixed with a fixed weight of the spent zeolite weighing of 0.125 g until obtaining a homogeneous solid mixture. Then, 1.5 mL of the activator solution was added to the solid mixture and handy mixed until it became a homogeneous paste. This paste was then transferred into a mold and solidified in an oven at 70°C for 24 h and allowed to cure for 7 d at room temperature. The zeolite-geopolymer samples and the spent zeolites were examined at extreme salinity and acidic environment

conditions by immersing them in 25 mL of H_2O, 0.1 M NaCl, and 0.5 M H_2SO_4 solutions for 10 d. The leachates were analyzed by ICP for any releasing heavy metal.

3. Results and discussion

3.1. Characterization of the synthesized zeolites

3.1.1. X-ray diffraction

The XRD patterns of NaY zeolite samples prepared from used aluminum foil as a cheap source of alumina are shown in Fig. 1. Analyzing the XRD patterns of the synthesized samples and comparing them with those of the commercial NaY zeolite leads to that aluminum foil can replace chemical grads sodium aluminates in the preparation of NaY zeolite. However, crystallization time was an important factor in the synthesis process. An insight look on the XRD patterns shows that the samples crystallized for 12 and 16 h at 100°C had several peaks which are irrelevant to the NaY zeolite phase at 12.53°, 17.63°, 21.68°, and 28.01°. Whilst, these peaks disappeared when crystallization time prolonged to 24 h at 100°C.

Fig. 2 shows the XRD of NaX zeolite prepared from an aluminum foil at 100°C and different crystallization time. Crystallizing the gel for 6 h produced an amorphous product and starting of appearing the main peaks of NaX zeolite at 2θ of 6.2°, 10.16°, 15.6°, 23.48°, 26.48°, 30.56°, 31.1°, and 32.24°. The comparison shows appearing several peaks that do not belong to NaX zeolite in the samples crystallized for 12 and 18 h at 12.44°, 17.69°, 21.71°, and 28.13°. While the sample crystallized for 24 h had an identical pattern to the pattern of the commercial NaX zeolite.

3.1.2. SEM and EDAX

Fig. 3 shows the SEM images of NaY zeolite samples prepared from used aluminum foil which will be used later to remove the heavy metals via ion-exchange
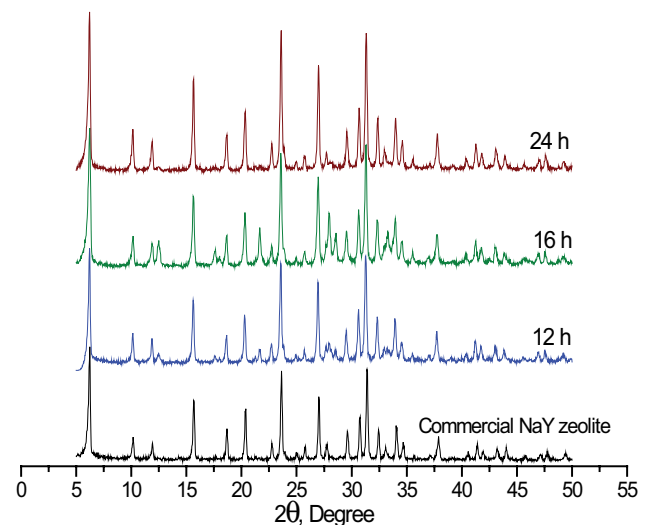
Fig. 1. XRD patterns of NaY zeolite prepared from aluminum foil at 100°C.

method. The images show that both samples crystallized for 12 and 16 h had undefined-form crystals. While a fully-crystallized sample was obtained when the gel was crystallized for 24 h at 100°C. Also, the SEM images revealed that the crystal size increased with increasing the crystallization time. These results are in good agreement with that obtained by Nouri et al. [52]. The EDAX results for a sample synthesized for 24 h at 100°C are shown in Fig. 4. The results emphasize that the sample has a Si/Al ratio of 2.28 and no impurities appeared within the NaY zeolite composition when the aluminum foil was utilized as a precursor. Also, the crystal properties presented in Table 1 show that this sample has an average crystal size calculated using ImageJ software of 1,566 nm.

SEM images of the synthesized NaX zeolite samples are shown in Fig. 5, where the morphology of samples crystallized for 12, 18, and 24 h were well-defined octahedral shape crystals. The same results were obtained by Zhang et al. [53]. The sample crystallized for 6 h gave a mixture of crystals and an amorphous product. Also, the images show the development of zeolite crystal size with

crystallization time. Where the crystal size reduced with increasing crystallization time. As confirmed by EDAX results shown in Fig. 4, no impurities appeared within the chemical composition of the NaX zeolite prepared from an aluminum foil at 100°C for 24 h. Also, this sample has a Si/Al ratio of 1.35 and an average crystal size of 1,596 nm as shown in Table 1. Both NaY zeolite and NaX zeolite samples which were obtained after 24 h of crystallization were selected to perform the ion-exchange process.

3.1.3. BET surface area

Table 1 shows that the BET surface area of NaY zeolite was 476.248 m²/g and it was 610.236 m²/g for NaX zeolite.

3.2. Removal of ions

The results of ion-exchange experiments conducted to remove individual metal ions by NaY zeolite and NaX zeolite were used further to conduct ion-exchange experiments to treat solutions containing binary and ternary metal ions. Figs. 7 and 8 present these results in term of ion-exchange capacity (q) which is represented by Eq. (2) and removal efficiency (%R) which is represented by Eq. (3):

$$q = \frac{\left(C_0 - C_{eq}\right) \times V}{W} \tag{2}$$

where q (mg/g) is the mass (mg) of metal ion removed per mass of zeolite W (g), V is the metal ion solution volume (L), C_0 and C_{eq} are the concentrations of the metal ion in solution (mg/L) initially and at equilibrium, respectively [4].

$$\%R = \frac{C_0 - C_t}{C_0} \times 100\% \tag{3}$$

where C_t is the concentrations of the metal ion in solution (mg/L) at any interval during the experiment time [54].

Fig. 6 shows the ion-exchange results obtained when NaY zeolite was used to remove Cd(II), Cu(II) and Hg(II) ions individually from their solutions. The results show that NaY zeolite has a stronger affinity toward Cd(II) and Cu(II)

Fig. 2. XRD patterns of NaX zeolite prepared from aluminum foil at 100°C.
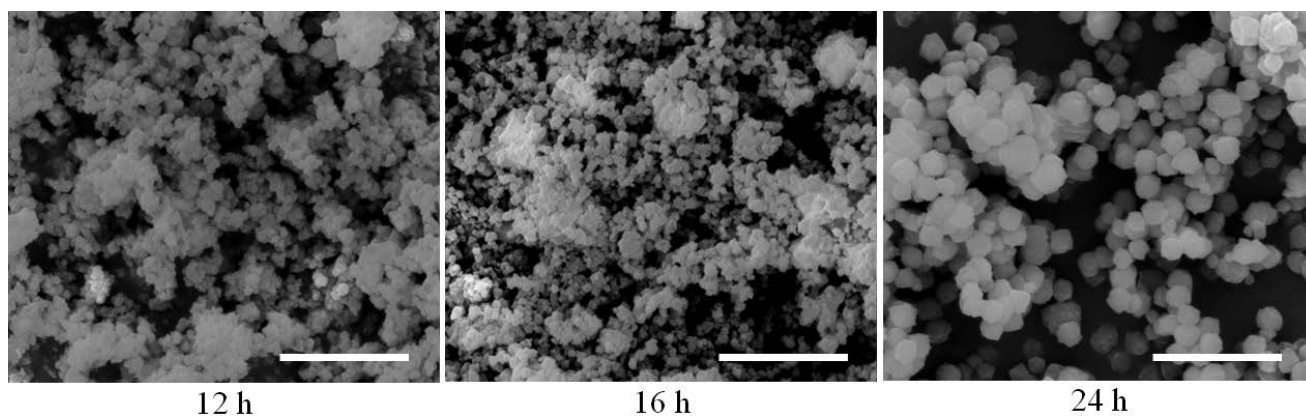
Fig. 3. SEM images of NaY zeolite prepared from aluminum foil at 100°C. The scale bar is 10 μm.
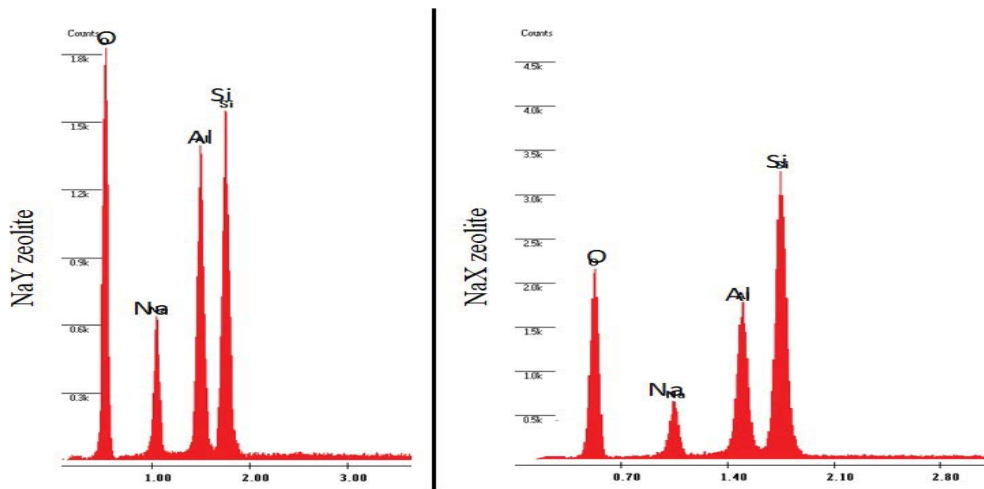
Fig. 4. EDAX results of the zeolites prepared from aluminum foil, crystallized at 100°C for 24 h.

Table 1
Crystal properties of NaY zeolite and NaX zeolite prepared from aluminum foil, crystallized at 100°C for 24 h

Zeolite type	Si/Al	Average crystal size (nm)	BET surface area (m^2/g)
NaY zeolite	2.28	1,566	476.248
NaX zeolite	1.35	1,596	610.236

ions than Hg(II) ion, thus NaY zeolite ion-exchange capacity was higher for Cd(II) and Cu(II) ions compared to Hg(II) ion (Fig. 6a). This sequence was reflected in the removal efficiency of Cd(II) and Cu(II) ions which was higher than of Hg(II) ion as illustrated in Fig. 6b. Therefore, the selectivity of NaY zeolite for the studied heavy metals was in the following order: Cd(II) > Cu(II) > Hg(II). Ahmed et al. [55] found that the exchange efficiency of Na-Y was in the order $Pb^{2+} > Cd^{2+} > Cu^{2+} > Zn^{2+} > Ni^{2+}$.
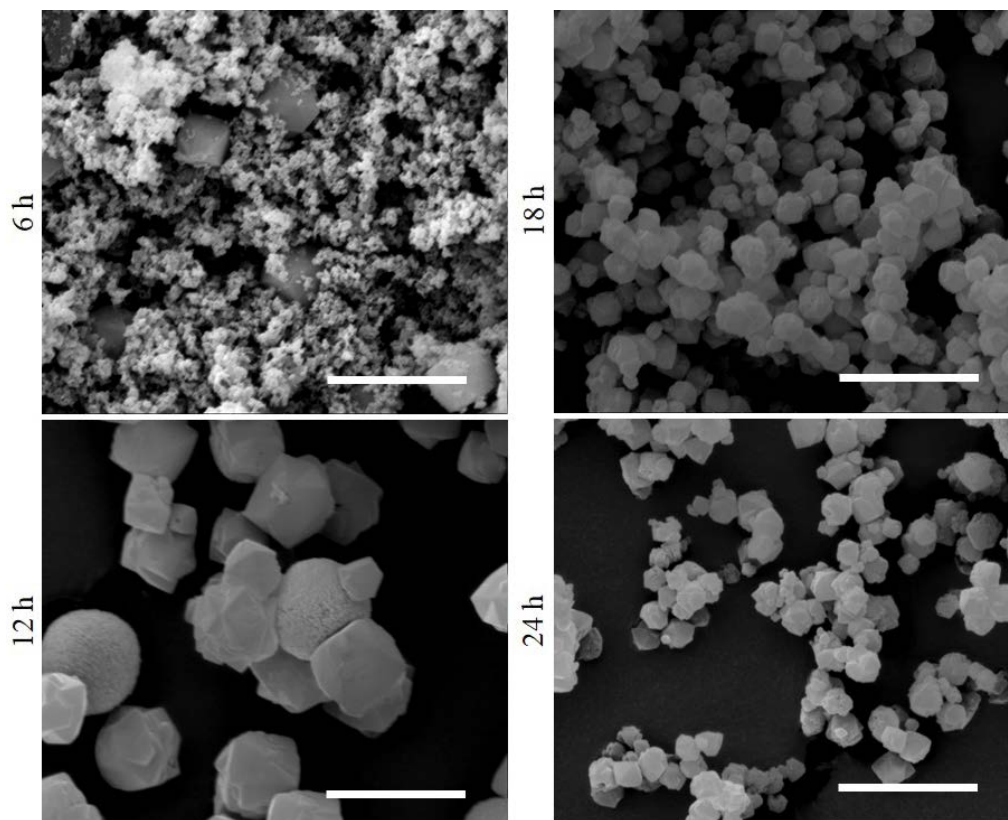
Fig. 5. SEM images of NaX zeolite prepared from aluminum foil at 100°C. The scale bar is 10 μm.
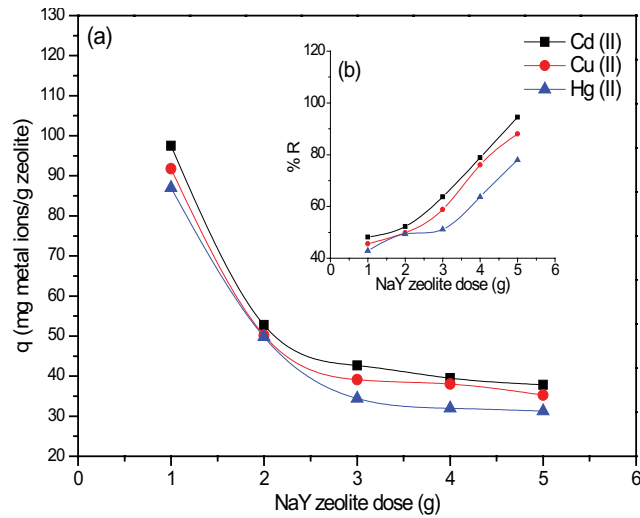
Fig. 6. (a) Ion-exchange capacity of NaY zeolite used to remove individual metal ions and (b) removal efficiency of the removed metal ions. $C_0 = 200$ ppm, $V = 1$ L, T_{room}, $S_{mix} = 200$ rpm, and $t_{eq} = 4$ h.
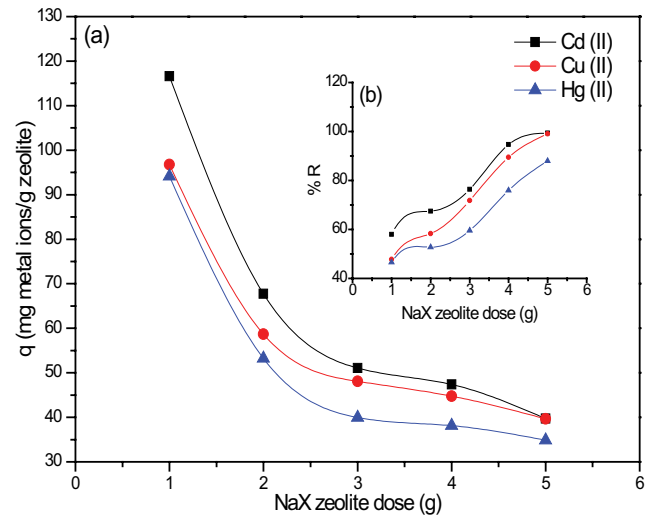
Fig. 7. (a) Ion-exchange capacity of NaX zeolite used to remove individual metal ions and (b) removal efficiency of the removed metal ions. $C_0 = 200$ ppm, $V = 1$ L, T_{room}, $S_{mix} = 200$ rpm, and $t_{eq} = 4$ h.

NaX zeolite showed similar behavior as NaY zeolite toward the removal of Cd(II), Cu(II) and Hg(II) ions from their solutions by ion-exchange as indicated in Fig. 7. In spite of the sensitivity of NaX zeolite structure toward the acidic solutions due to its low Si/Al ratio, it gave higher ion-exchange capacity than NaY zeolite as shown in Fig. 7a. These results were confirmed by the pH readings of the solutions recorded at the end of the ion-exchange as shown in Table 2. High pH values at the end of the ion-exchange process using NaX zeolites indicated the high ion-exchange rate leading to form sodium hydroxide. Also, Ibrahim et al. [1], found that the selectivity sequence of A and X zeolite was Pb²⁺ > Cd²⁺ > Cu²⁺ > Zn²⁺ > Ni²⁺.

The charge, ionic radii, and consequently hydrated radii of the exchanging ions play a dominant role in the ion-exchange process [56]. Where, the ionic radii of Cd(II) is 0.97 Å, Cu(II) is 0.72 Å [57] and Hg(II) is 0.69 Å [58,59]. For the same electronic charge, the larger the ionic radii (the smaller hydrated radii) greater the tendency for adsorption or exchange [56,60]. This fact reflects that Hg(II)

with a small ionic radius has a powerful propensity to stay in a solution, therefore it is weakly exchanged or adsorbed on the surface of the zeolite. Unlike, Cd(II) and Cu(II) that showed a strong tendency for ion-exchange and thus higher removal efficiency was obtained. Furthermore, the overview given by Figs. 6 and 7 is that the ion-exchange capacity of both NaY zeolite and NaX zeolite reduced with increasing zeolite dose. This can be explained by the mathematical relation between zeolite amounts and capacity value illustrated in Eq. (2). This Eq. (2) indicates an inverse relationship between the zeolite dosage and the capacity value even though the large difference between the initial and remaining concentrations obtained at this dose.

Table 2 displays the pH of the solutions containing individual, binary, and ternary metal ions before and after ion-exchange with NaY zeolite and NaX zeolite. It is worth noting that the solutions of the three individual metals were initially acidic. But, the solutions became more acidic when they contained more than one metal ions, especially when one of those metals were mercury (Hg(II)).

Table 2
pH of the solutions containing individual, binary and ternary metal ions of Cd(II), Cu(II) and Hg(II) with $C_0 = 200$ ppm before and after ion-exchange with NaY zeolite and NaX zeolite

| Heavy metal present | Initial pH | pH of the metal solutions after 24 h of ion-exchange | | | | | | | | | |
| | | NaY zeolite | | | | | NaX zeolite | | | | |
		1 g/L	2 g/L	3 g/L	4 g/L	5 g/L	1 g/L	2 g/L	3 g/L	4 g/L	5 g/L
Cd	5.19	6.12	7.01	7.31	7.44	7.60	6.12	6.86	7.12	7.25	7.64
Cu	4.12	5.20	5.48	6.01	6.38	6.54	5.49	6.62	7.40	7.70	7.57
Hg	3.15	6.23	6.67	6.75	6.82	6.88	6.58	7.11	7.13	7.30	7.59
Cd + Cu	4.97	–	–	–	–	6.02	–	–	–	–	6.43
Cd + Hg	3.13	–	–	–	–	6.26	–	–	–	–	6.88
Cu + Hg	3.07	–	–	–	–	5.58	–	–	–	–	6.87
Cd + Cu + Hg	3.11	–	–	–	–	5.08	–	–	–	–	6.26

Since, the pH of all solutions containing Hg(II) ions did not raised above 3.15. The results presented in Table 2 shows that the pH of the solutions significantly raised at the end of the ion-exchange time due to occurring ion-exchange between the heavy metal ions and the cations (Na⁺) that occupy the zeolite framework.

The results showing the behavior of the synthesized NaY zeolite and NaX zeolite in the ion-exchange process to treat solutions containing binary and ternary metal ions are displayed in Figs. 8 and 9, respectively. For solutions containing binary metals, the metals showed the same selectivity order toward both zeolites which is Cd(II) > Cu(II) > Hg(II). When NaY zeolite was used to remove Cd(II) and Cu(II) from solutions containing binary and ternary metals, NaY zeolite showed convergent removal efficiency for these metal ions (see Fig. 8a and d). But when NaX zeolite was used for a solution containing ternary metals, the order varied as Cu(II) > Cd(II) > Hg(II) (Fig. 9d). These results are supported by the EDAX results presented in Tables 3 and 4 of the spent NaY and NaX zeolites for ion-exchange with Cd(II), Cu(II) and Hg(II) ions. Also, the results of EDAX that show the appearance of peaks of Cd(II), Cu(II) and Hg(II) within the elemental analysis of the spent NaY and NaX zeolites are displayed in Figs. 10 and 11, respectively. These results clearly show that the percentage of Cd(II) was very close to the percentage of Cu(II) ions present in NaY zeolite and NaX zeolite used for solutions containing both metals as well from solutions containing ternary metals. In the same context, the percentage of Hg(II) ions present within the spent zeolites was obviously lower than the percentage of Cd(II) and Cu(II) ions when they present in binary or ternary solutions.

A comparison made based on the zeolite type shows that the %R of the metals was higher for NaX zeolite than NaY. This can be attributed to the structural properties of NaX such as lower Si/Al ratio (which provides high cations concentration to exchange) and larger surface area.

The reading of solution pH presented in Table 2 show that the pH of the binary and ternary metals solutions did not raise as much as raised in the case of solutions containing individual metals. This can be attributed to the competition among the different metal ions on the same dose of zeolites that reduced the ion-exchange rate and less sodium hydroxide formed.

3.3. Kinetics models

Studying the ion-exchange kinetics leads to a good understanding of the rate of the process and provided information for the process design [61]. The kinetics of the removal of metal ions from binary and ternary solutions was studied using the pseudo-first-order (Lagergren equation) given by Eq. (4) and pseudo-second-order models given by Eq. (5) [62]:

$$\frac{dq_t}{dt} = k_1 \left(q_e - q_t \right) \tag{4}$$

$$\frac{dq_t}{dt} = k_2 \left(q_e - q_t \right)^2 \tag{5}$$

These equations were solved by integration and substituting the boundary conditions of $t = 0$ to $t = t$, and $q_t = 0$ to $q_t = q_t$. The experimental data were applied in the linearized
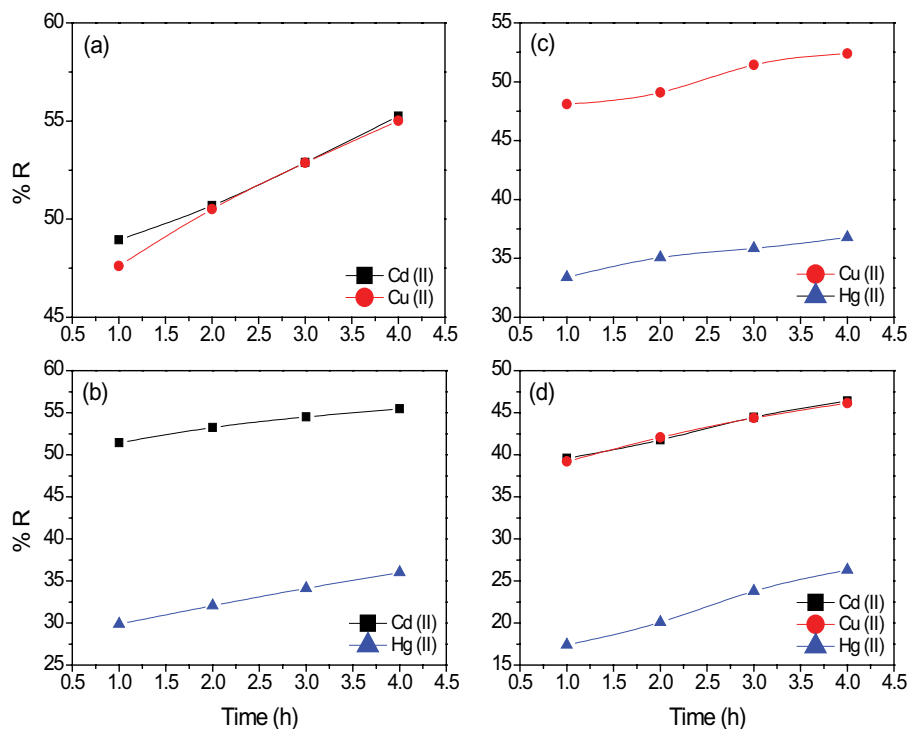
Fig. 8. Removal efficiency of the removed metal ions by NaY zeolite from solutions containing binary and ternary metal ions. C_0 = 200 ppm, W = 5 g, V = 1 L, T_{room}, and mixing speed = 200 rpm.
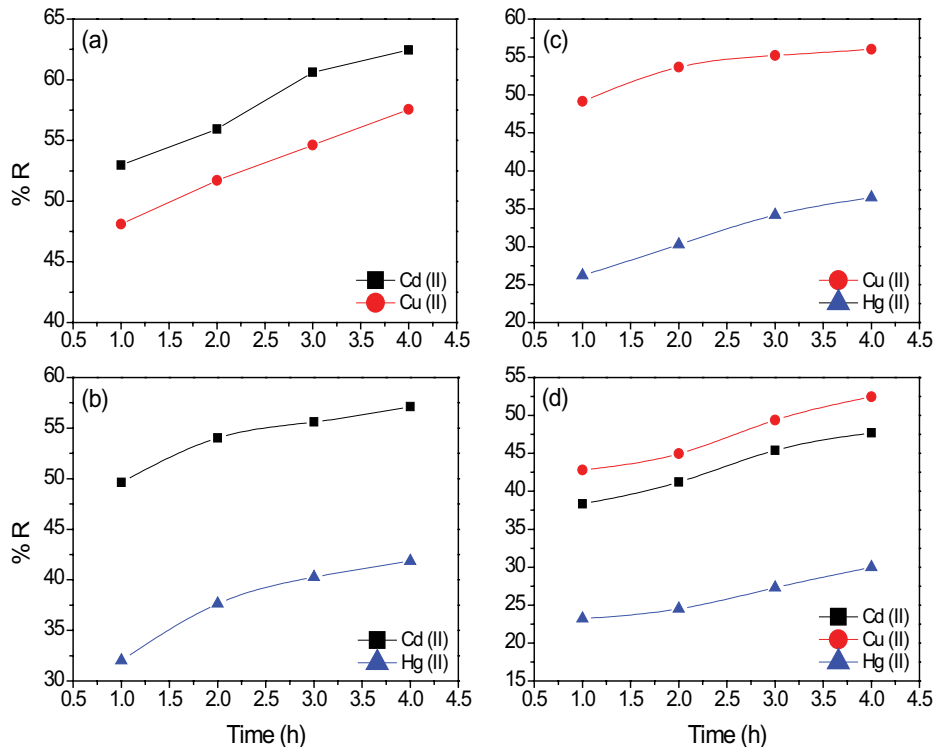
Fig. 9. Removal efficiency of the removed metal ions by NaX zeolite from solutions containing binary and ternary metal ions. C_0 = 200 ppm, W = 5 g, V = 1 L, T_{room}, and mixing speed = 200 rpm.

Table 3
EDAX results of NaY zeolite before and after ion-exchange with Cd(II), Cu(II) and Hg(II) ions in the form of weight percent of each element

Element	NaY zeolite before ion-exchange	NaY zeolite after ion-exchange for heavy metals removal						
		Cd ion removal	Cu ion removal	Hg ion removal	Cd, Cu ion removal	Cd, Hg ion removal	Cu, Hg ion removal	Cd, Cu, Hg ion removal
O	43.76%	42.23%	44.25%	41.94%	48.10%	46.58%	46.58%	46%
Na	7.73%	6.01%	5.24%	7.70%	3.76%	6.56%	3.91%	2.88%
Al	14.78%	14.46%	14.38%	15.14%	12.90%	14.17%	13.46%	13.15%
Si	33.73%	28.94%	28.35%	32.10%	27.74%	28.52%	29.70%	28.67%
Cd	–	8.94%	–	–	3.63%	3.66%	–	4.32%
Cu	–	–	7.78%	–	3.87%	–	5.36%	4.43%
Hg	–	–	–	3.11%	–	0.51%	0.89%	0.56%

form of the integrated equations given by Eq. (6) (for the first-order) and Eq. (7) (for the second-order) to investigate the ion-exchange kinetics [61].

$$\log(q_e - q_t) = \log q_e - \left(\frac{k_1}{2.303}\right)t \qquad (6)$$

$$\frac{t}{q_t} = \frac{1}{k_2 \cdot q_e^2} + \frac{t}{q_e} \qquad (7)$$

The first-order rate constant (k_1 s^{-1}), second-order rate constant (k_2 g/mg s), and q_e were estimated according to

intercepts and slopes of the linear plots shown in Figs. 12 and 13 and summarized in Tables 5 and 6. The results presented in these figures and table show that the pseudo-first-order model did not confirm the experimental results with much varied computed values of q_e. Also, the kinetics model results show that the results of ion-exchange of the studied metal ions were best adapted to the pseudo-second-order model. This is because the pseudo-second-order model gave higher correlation coefficients (R^2 = 0.9675–1) and close estimated values of q_e to the experimental values. These findings elucidate that the mechanism of ion-exchange by both NaY zeolite and NaX zeolite with binary and ternary metals solutions is

Table 4
EDAX results of NaX zeolite before and after ion-exchange with Cd(II), Cu(II) and Hg(II) ions in the form of weight percent of each element

Element	NaX zeolite before ion-exchange	NaX zeolite after ion-exchange for heavy metals removal						
		Cd ion removal	Cu ion removal	Hg ion removal	Cd and Cu ion removal	Cd and Hg ion removal	Cu and Hg ion removal	Cd, Cu and Hg ion removal
O	45.45%	39.14%	44.53%	46.63%	45.81%	40.87%	44.25%	42%
Na	9.83%	7.57%	7.63%	8.25%	5.77%	8.35%	6.88%	4.57%
Al	19.06%	16.87%	17.85%	16.67%	16%	16.96%	17.81%	17.1%
Si	25.67%	27.13%	23.89%	26.11%	23.89%	27.67%	24.26%	24.47%
Cd	–	9.3%	–	–	4.15%	4.98%	–	5.25%
Cu	–	–	6.12%	–	4.36%	–	5.18%	5.46%
Hg	–	–	–	2.33%	–	1.16%	1.58%	1.15%
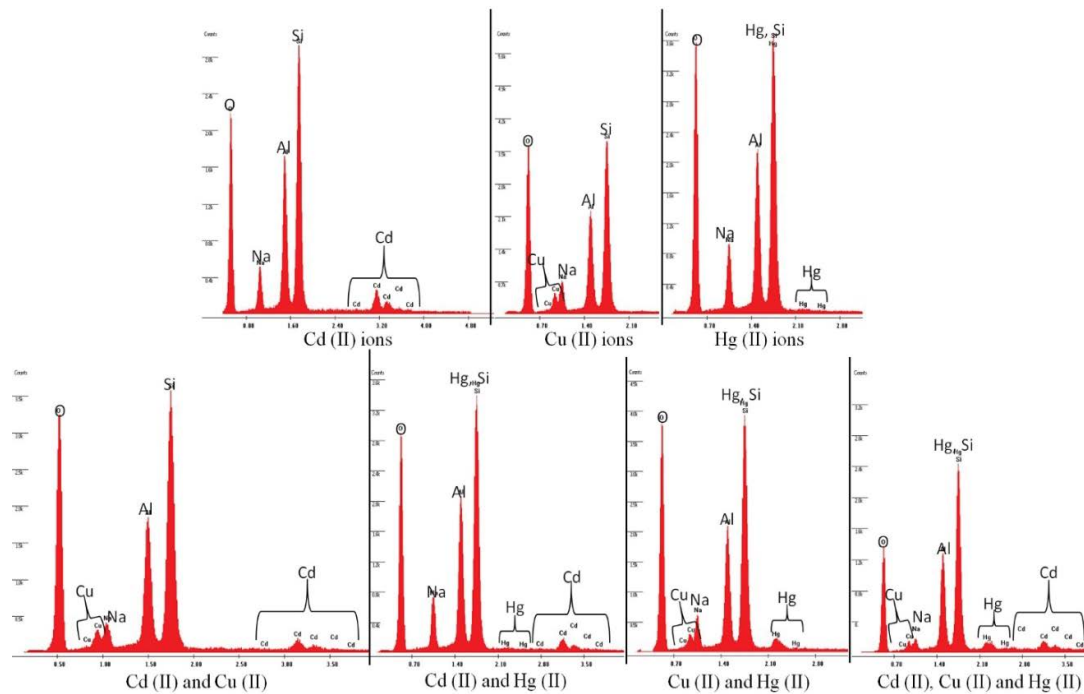
Fig. 10. EDAX results of NaY zeolite after ion-exchange with solutions containing individual, binary, and ternary metal ions.

Table 5
The parameters of the pseudo-first-order model of ion-exchange by NaY zeolite and NaX zeolite with binary and ternary metals solutions

	Kinetic parameters	Metal ions								
		Cd in Cd/Hg	Hg in Cd/Hg	Cu in Cu/Hg	Hg in Cu/Hg	Cd in Cd/Cu	Cu in Cd/Cu	Cd in Cd/Cu/Hg	Cu in Cd/Cu/Hg	Hg in Cd/Cu/Hg
NaY zeolite	k_1 (s^{-1})	0.056	0.041	0.051	0.040	0.038	0.041	0.049	0.035	0.035
	$q_{e\text{-Model}}$ (mg/g)	104.689	46.750	81.115	29.349	50.246	62.503	90.033	38.045	35.925
	$q_{e\text{-Experimental}}$ (mg/g)	22.285	14.616	21.155	13.752	22.003	22.580	18.079	18.817	10.441
NaX zeolite	k_1 (s^{-1})	0.045	0.123	0.057	0.040	0.057	0.050	0.045	0.038	0.025
	$q_{e\text{-Model}}$ (mg/g)	71.713	8013.090	121.899	58.103	194.715	126.853	85.487	62.345	19.498
	$q_{e\text{-Experimental}}$ (mg/g)	22.656	16.639	22.207	14.497	24.781	22.827	18.919	20.807	11.910
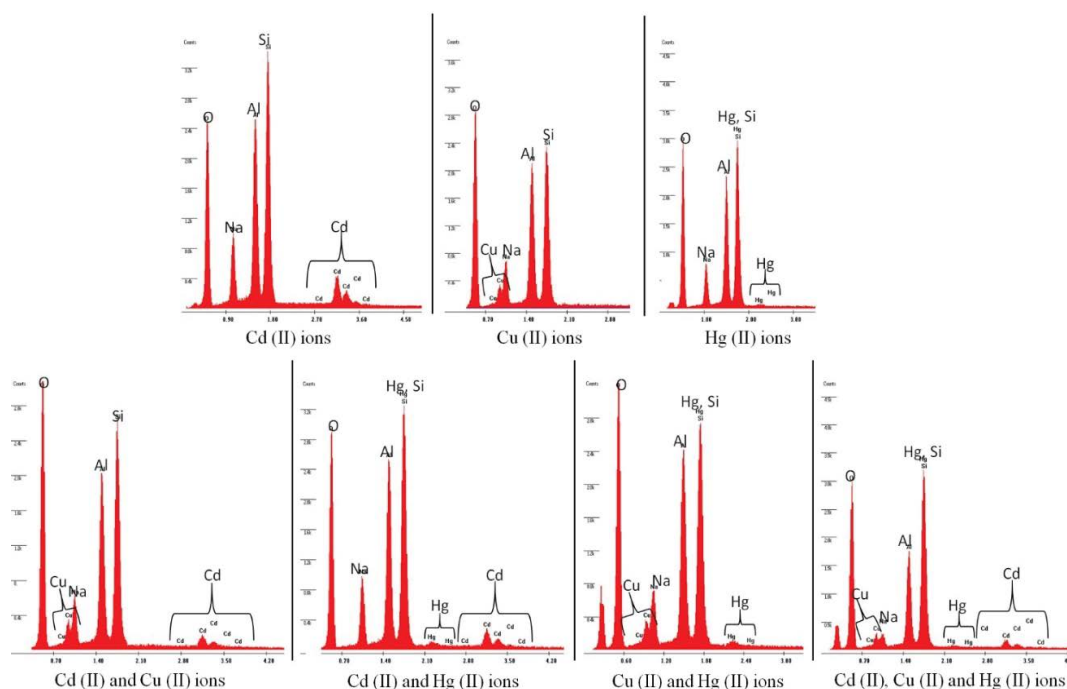
Fig. 11. EDAX results of NaX zeolite after ion-exchange with solutions containing individual, binary, and ternary metal ions.

Table 6
The parameters of the pseudo-second-order model of ion-exchange by NaY zeolite and NaX zeolite with binary and ternary metals solutions

	Kinetic parameters	Metal ions solution								
		Cd in Cd/Hg	Hg in Cd/Hg	Cu in Cu/Hg	Hg in Cu/Hg	Cd in Cd/Cu	Cu in Cd/Cu	Cd in Cd/ Cu/Hg	Cu in Cd/ Cu/Hg	Hg in Cd/ Cu/Hg
NaY zeolite	k_2 (s^{-1})	0.0157	0.0024	0.0128	0.0178	0.0080	0.0086	0.0078	0.0085	0.0047
	$q_{e\text{-Model}}$ (mg/g)	22.321	14.663	21.231	13.793	22.624	21.978	18.149	18.904	10.650
	$q_{e\text{-Experimental}}$ (mg/g)	22.285	14.616	21.155	13.752	22.003	22.580	18.079	18.817	10.441
NaX zeolite	k_2 (s^{-1})	0.0087	0.0055	0.010	0.0046	0.0056	0.0059	0.0054	0.0051	0.0068
	$q_{e\text{-Model}}$ (mg/g)	22.831	16.949	22.422	14.771	25	22.883	19.084	20.877	11.891
	$q_{e\text{-Experimental}}$ (mg/g)	22.656	16.639	22.207	14.497	24.781	22.827	18.919	20.807	11.910

controlled by chemisorption. Since the chemical reaction of metal ions with the ion-exchange sites is the rate-limiting step, the ion-exchange kinetics of metal ions are compatible with the postulation of the pseudo-second-order model as confirmed by the findings of [7,63]. Moreover, the close values of k_2 for both Cd(II) ions and Cu(II) ions present together in the binary and ternary metal solutions are the reason behind obtaining close %R values of both metals using NaY zeolite and NaX zeolite and obtaining close ion-exchange capacities.

3.4. Solidification

Tables 7 and 8 display the concentration of the studied heavy metals that leached from the spent NaY zeolite and NaX zeolite respectively after 10 d of immersion in H$_2$O, 0.1 N NaCl solution, and 0.5 M H$_2$SO$_4$ solution. Where the concentration released to water is considerably less than the concentration released to the salty and acidic solution. This is because NaCl provided appropriate cations for another ion-exchange process causing the capturing of Na cation by zeolites and releasing the hosted metal ions. The results of all solidified samples immersed in H$_2$O show the low leaching of metal ions to water during the test time. The concentration of metal ions leached was: 0.003–0.0045 ppm for Cd(II) ions, 0.001–0.0022 ppm for Cu(II) ions, and 0.00048–0.0021 ppm for Hg(II) ions. Whilst, the concentration of metal ions leached to 0.1 M NaCl solution was: 0.392–0.591 ppm for Cd(II) ions, 0.212–0.503 ppm for Cu(II) ions, and 0.163–0.542 ppm for Hg(II) ions.

Also, the acidic media decomposes the structure of the low Si/Al zeolites that bearing the removed heavy metals through leaching of Al species from the zeolite structure. Due to the high sensitivity of zeolite to acidic conditions, the stability of the solidified metals-bearing zeolites was examined by immersing them in a 0.5 M H$_2$SO$_4$ solution
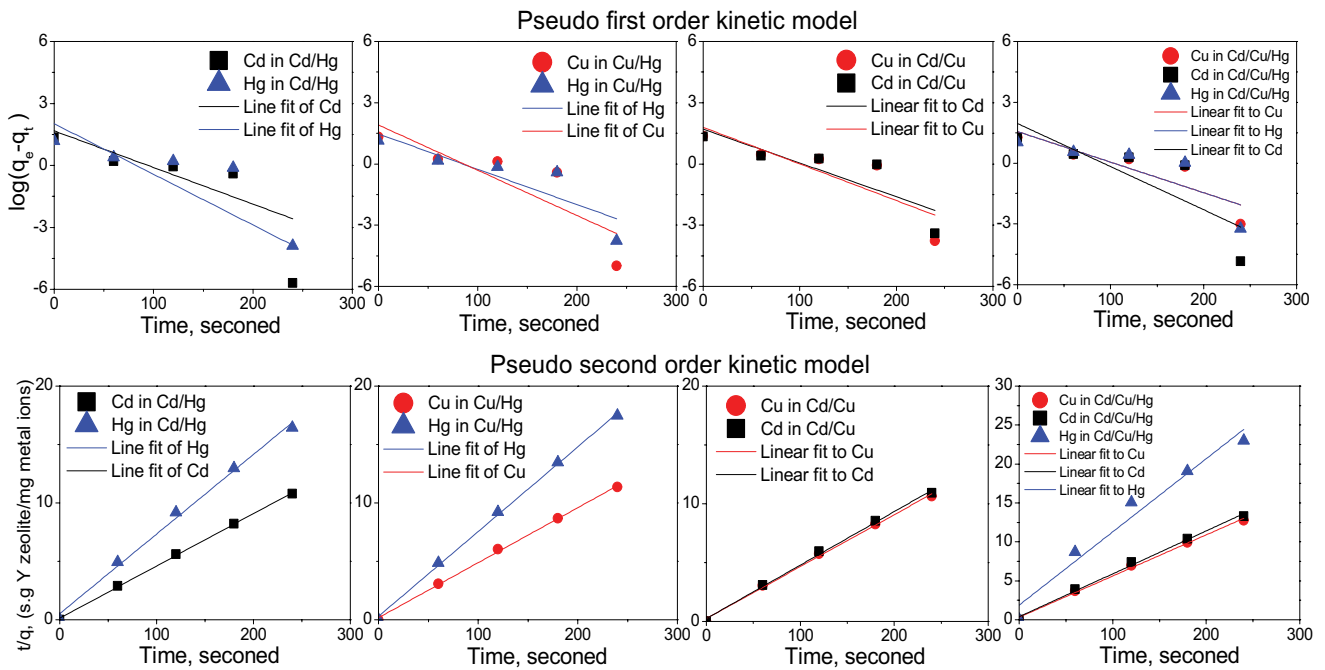
Fig. 12. Linear plots of the kinetic models of ion-exchange by NaY zeolite with binary and ternary metals solutions.
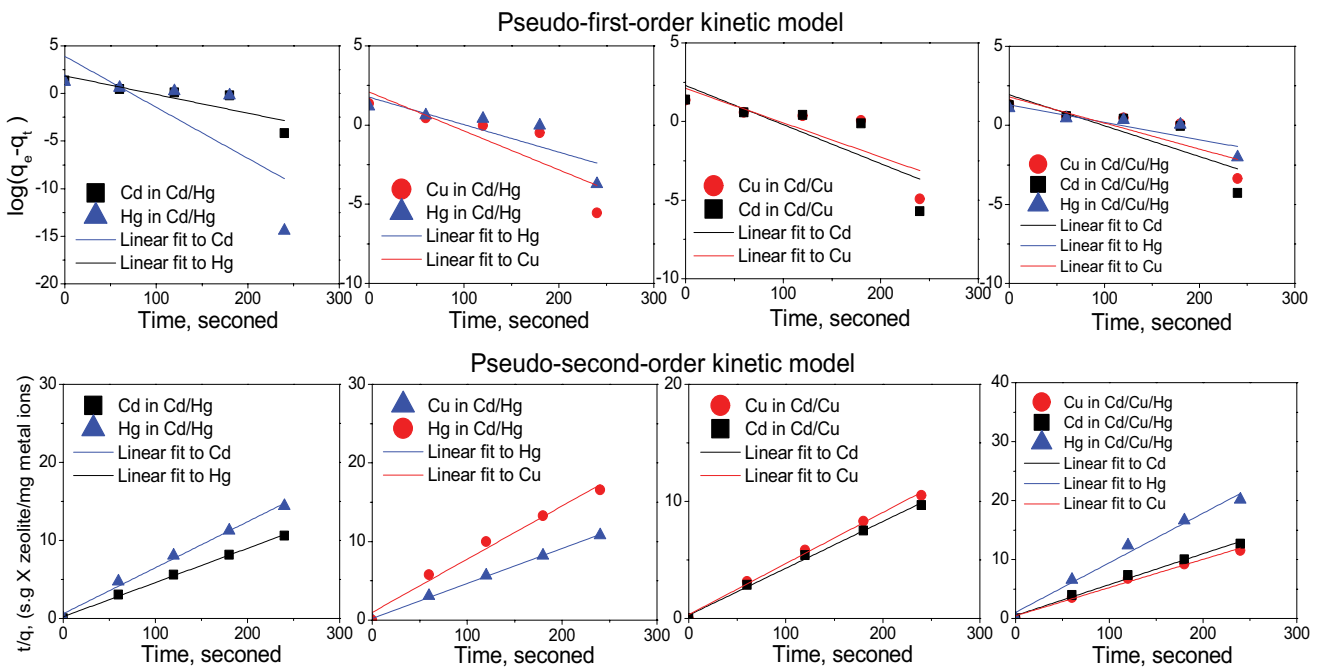
Fig. 13. Linear plots of the kinetic models of ion-exchange by NaX zeolite with binary and ternary metals solutions.

for 10 d. Tables 9 and 10 display the obtained results for different cement: fly ash ratios. Less concentration of metal ions leached to the H_2SO_4 solution when the geopolymer was prepared with a ratio of 1 cement: 3 fly ash which can be attributed to the fly ash nature of forming more sticky consistency. Geopolymerization succeeded in reducing the concentration of leached metal ions to the acidic medium (H_2SO_4 solution) by about 98%. However, more intensive work is required in this frame of work to reduce the concentration of metals leached from the solidified zeolites. This is because the concentration of the leached metal ions to salty and acidic mediums did not meet the requirement of the United States Environmental Protective Agency (EPA) in 2009. Where, this requirement identified 0.005 ppm for Cd(II), 1.3 ppm for Cu(II) and 0.002 ppm for Hg(II) as allowable concentrations in drinking water [56].

Table 7
Concentration of heavy metal ions leached from spent NaY zeolite before solidification

Spent zeolite case	Cd ions concentration (ppm)	Cu ions concentration (ppm)	Hg ions concentration (ppm)	Cd and Cu ions concentration (ppm)		Cd and Hg ions concentration (ppm)		Cu and Hg ions concentration (ppm)		Cd, Cu, and Hg ions concentration (ppm)		
				Cd	Cu	Cd	Hg	Cu	Hg	Cd	Cu	Hg
Immersed in H$_2$O	0.143	0.109	0.063	0.120	0.134	0.115	0.049	0.071	0.143	0.139	0.140	0.032
Immersed in 0.1 M NaCl	31.887	29.338	23.206	18.864	19.642	24.479	9.311	8.849	17.765	14.788	16.237	6.687
Immersed in 0.5 M H$_2$SO$_4$	68.124	62.428	43.454	42.817	48.333	59.367	31.089	61.845	26.428	43.648	40.222	21.645

Table 8
Concentration of heavy metal ions leached from spent NaX zeolite before solidification

Spent zeolite case	Cd ions concentration (ppm)	Cu ions concentration (ppm)	Hg ions concentration (ppm)	Cd and Cu ions concentration (ppm)		Cd and Hg ions concentration (ppm)		Cu and Hg ions concentration (ppm)		Cd, Cu, and Hg ions concentration (ppm)		
				Cd	Cu	Cd	Hg	Cu	Hg	Cd	Cu	Hg
Immersed in H$_2$O	0.201	0.189	0.081	0.148	0.151	0.132	0.044	0.090	0.161	0.170	0.173	0.041
Immersed in 0.1 M NaCl	36.122	34.084	24.631	21.439	21.880	19.016	13.324	10.112	18.046	15.106	17.247	10.449
Immersed in 0.5 M H$_2$SO$_4$	73.238	67.727	48.172	48.667	44.785	63.219	40.606	64.111	34.864	42.218	50.648	26.334

Table 9
Concentration of heavy metal ions leached from the solidified NaY zeolite to 0.5 M H$_2$SO$_4$ after 10 d

Solidified samples	Cd ions concentration (ppm)	Cu ions concentration (ppm)	Hg ions concentration (ppm)	Cd and Cu ions concentration (ppm)		Cd and Hg ions concentration (ppm)		Cu and Hg ions concentration (ppm)		Cd, Cu, and Hg ions concentration (ppm)		
				Cd	Cu	Cd	Hg	Cu	Hg	Cd	Cu	Hg
3 Cement:1 fly ash	1.213	1.448	1.747	1.321	1.421	1.604	1.828	0.812	0.879	1.103	1.337	1.214
1 Cement:1 fly ash	1.467	1.212	1.945	1.603	1.146	1.830	1.865	0.679	0.648	1.333	1.011	1.104
1 Cement:3 fly ash	1.265	1.365	1.603	0.867	0.844	1.430	1.514	0.968	0.745	1.289	0.833	0.744
Commercial cement	1.704	0.906	2.113	1.455	1.121	1.643	2.245	0.949	1.668	0.946	0.711	1.400

Table 10
Concentration of heavy metal ions leached from the solidified NaY zeolite to 0.5 M H$_2$SO$_4$ after 10 d

Solidified samples	Cd ions concentration (ppm)	Cu ions concentration (ppm)	Hg ions concentration (ppm)	Cd and Cu ions concentration (ppm)		Cd and Hg ions concentration (ppm)		Cu and Hg ions concentration (ppm)		Cd, Cu and Hg ions concentration (ppm)		
				Cd	Cu	Cd	Hg	Cu	Hg	Cd	Cu	Hg
3 Cement:1 fly ash	1.583	1.431	1.866	0.785	1.610	0.810	1.613	0.879	1.574	0.912	1.060	1.103
1 Cement:1 fly ash	1.463	1.501	1.833	0.766	1.501	0.946	1.585	0.910	1.436	0.886	0.746	0.870
1 Cement:3 fly ash	1.212	1.320	1.337	0.760	1.428	0.801	1.468	0.899	1.311	0.611	0.468	0.682
Commercial cement	1.621	1.445	2.032	0.831	1.545	0.883	1.666	1.213	1.608	0.827	1.124	1.334

4. Conclusions

The outcomes of this work show that aluminum foil can be successfully used as an inexpensive alumina source to prepare pure phase NaY zeolite and NaX zeolite by a conventional hydrothermal method at 100⁰C for 24 h. Both prepared zeolites confirmed their ability for removing a combination of heavy metals with different ionic radii and boiling points, whereas NaX zeolite gave higher ion-exchange capacity than NaY zeolite. However, the order of the selectivity sequence of the studied metal ions varied according to the zeolite type and the number of metals present in the solution being treated. The ion-exchange results highly adapted to the pseudo-second-order kinetic model with $R^2 = 0.96–1$ which confirms the ion-exchange process was controlled by the chemisorption. Also, geopolymers made of 1 cement:3 fly ash ratio successfully diminished the leachate concentration in the acidic solution to an acceptable level.

References

[1] H.S. Ibrahim, T.S. Jamil, E.Z. Hegazy, Application of zeolite prepared from Egyptian kaolin for the removal of heavy metals: II. Isotherm models, J. Hazard. Mater., 182 (2010) 842–847.
[2] S.M.A. Jubouri, H.A. Sabbar, H.A. Lafta, B.I. Waisi, Effect of synthesis parameters on the formation 4A zeolite crystals: characterization analysis and heavy metals uptake performance study for water treatment, Desal. Water Treat., 165 (2019) 290–300.
[3] S.M. Shaheen, F.I. Eissa, K.M. Ghanem, H.M.G.E. Din, F.S.A. Anany, Heavy metals removal from aqueous solutions and wastewaters by using various byproducts, J. Environ. Manage., 128 (2013) 514–521.
[4] S.M.A. Jubouri, S.M. Holmes, Immobilization of cobalt ions using hierarchically porous 4A zeolite-based carbon composites: ion-exchange and solidification, J. Water Process Eng., 33 (2020) 101059, doi: 10.1016/j.jwpe.2019.101059.
[5] S. Kocaoba, Adsorption of Cd(II), Cr(III) and Mn(II) on natural sepiolite, Desalination, 244 (2009) 24–30.
[6] A. Adamczuk, D. Kołodyńska, Equilibrium, thermodynamic and kinetic studies on removal of chromium, copper, zinc and arsenic from aqueous solutions onto fly ash coated by chitosan, Chem. Eng. J., 274 (2015) 200–212.
[7] D. Ferhat, D. Nibou, M. Elhadj, S. Amokrane, Adsorption of Ni²⁺ ions onto NaX and NaY zeolites: equilibrium, kinetics, intra crystalline diffusion and thermodynamic studies, Iran. J. Chem. Chem. Eng., 38 (2019) 63–81.
[8] A.H. Sulaymon, B.A. Abdulmajeed, A.B. Salman, Electrochemical removal of cadmium from simulated wastewater using a smooth rotating cylinder electrode, Desal. Water Treat., 54 (2015) 2557–2563.
[9] A.H. Sulaymon, B.A. Abdulmajeed, A.B. Salman, Removal of cadmium from simulated wastewater by using stainless steel concentric tubes electrochemical reactor, Desal. Water Treat., 68 (2017) 220–225.
[10] H. Javadian, F. Ghorbani, H.A. Tayebi, S.H. Asl, Study of the adsorption of Cd(II) from aqueous solution using zeolite-based geopolymer, synthesized from coal fly ash; kinetic, isotherm and thermodynamic studies, Arabian J. Chem., 8 (2015) 837–849.
[11] R.T. Hadi, A.B. Salman, S. Nabeel, S.A. Soud, Recovery of lead from simulated wastewater by using stainless steel rotating cylinder electrode electrochemical reactor, Desal. Water Treat., 99 (2017) 266–271.
[12] M.R. Awual, M.M. Hasan, G.E. Eldesoky, M.A. Khaleque, M.M. Rahman, M. Naushad, Facile mercury detection and removal from aqueous media involving, Chem. Eng. J., 290 (2016) 243–251.

[13] M. Ahmaruzzaman, Industrial wastes as low-cost potential adsorbents for the treatment of wastewater laden with heavy metals, Adv. Colloid Interface Sci., 166 (2011) 36–59.

[14] M.A. Shavandi, Z. Haddadian, M.H.S. Ismail, N. Abdullah, Z.Z. Abidin, Removal of Fe(III), Mn(II) and Zn(II) from palm oil mill effluent (POME) by natural zeolite, J. Taiwan Inst. Chem. Eng., 43 (2012) 750–759.

[15] Z.A. Husoon, Investigation biosorption potential of copper and lead from industrial waste- water using orange and lemon peels, J. Al-Nahrain Univ., 16 (2013) 173–179.

[16] M. Kapur, M.K. Mondal, Competitive sorption of Cu(II) and Ni(II) ions from aqueous solutions: kinetics, thermodynamics and desorption studies, J. Taiwan Inst. Chem. Eng., 45 (2014) 1803–1813.

[17] J.A. Alexander, A. Surajudeen, E.U. Aliyu, A.U. Omeiza, M. Abbas, A. Zaini, Multi metals column adsorption of lead(II), cadmium(II) and manganese(II) onto natural bentonite clay, Water Sci. Technol., 76 (2017) 2232–2241.

[18] V.C.T. Costodes, H. Fauduet, C. Porte, A. Delacroix, Removal of Cd(II) and Pb(II) ions, from aqueous solutions, by adsorption onto sawdust of *Pinus sylvestris*, J. Hazard. Mater., 105 (2003) 121–142.

[19] R. Han, W. Zou, H. Li, Y. Li, J. Shi, Copper(II) and lead(II) removal from aqueous solution in fixed-bed columns by manganese oxide coated zeolite, J. Hazard. Mater., 137 (2006) 934–942.

[20] W. Qiu, Y. Zheng, Removal of lead, copper, nickel, cobalt, and zinc from water by a cancrinite-type zeolite synthesized from fly ash, Chem. Eng. J., 145 (2009) 483–488.

[21] B. Alyüz, S. Veli, Kinetics and equilibrium studies for the removal of nickel and zinc from aqueous solutions by ion exchange resins, J. Hazard. Mater., 167 (2009) 482–488.

[22] G. Sharma, B. Thakur, A. Kumar, S. Sharma, M. Naushad, F.J. Stadler, Atrazine removal using chitin-cl-poly(acrylamide-co-itaconic acid) nanohydrogel: isotherms and pH responsive nature, Carbohydr. Polym., 241 (2020) 116258, doi: 10.1016/j.carbpol.2020.116258.

[23] M. Zhang, P. Gu, Z. Zhang, J. Liu, L. Dong, G. Zhang, Effective, rapid and selective adsorption of radioactive Sr²⁺ from aqueous solution by a novel metal sulfide adsorbent, Chem. Eng. J., 351 (2018) 668–677.

[24] A. Mittal, M. Naushad, G. Sharma, Z.A. Alothman, S.M. Wabaidur, M. Alam, Fabrication of MWCNTs/ThO₂ nanocomposite and its adsorption behavior for the removal of Pb(II) metal from aqueous medium, Desal. Water Treat., 57 (2015) 21863–21869.

[25] X. Tan, M. Fang, X. Wang, Preparation of TiO₂/multiwalled carbon nanotube composites and their applications in photocatalytic reduction of Cr(VI) study, J. Nanosci. Nanotechnol., 8 (2008) 5624–5631.

[26] G. Sharma, M. Naushad, Adsorptive removal of noxious cadmium ions from aqueous medium using activated carbon/zirconium oxide composite: Isotherm and kinetic modelling, J. Mol. Liq., 310 (2020) 113025, doi: 10.1016/j.molliq.2020.113025.

[27] T.W. Chen, A. Sivasamy Vasantha, S.M. Chen, D.A. Al Farraj, M.S. Elshikh, R.M. Alkufeidy, M.M.A. Khulaifi, Sonochemical synthesis and fabrication of honeycomb like zirconium dioxide with chitosan modified electrode for sensitive electrochemical determination of anti-tuberculosis (TB) drug, Ultrason. Sonochem., 59 (2019) 104718, doi: 10.1016/j.ultsonch.2019.104718.

[28] A.M.E. Kamash, Evaluation of zeolite A for the sorptive removal of Cs⁺ and Sr²⁺ ions from aqueous solutions using batch and fixed bed column operations, J. Hazard. Mater., 151 (2008) 432–445.

[29] Inamuddin, M. Luqman, Ion Exchange Technology I, 2012, Springer, Netherlands.

[30] D.A.H.D. Rio, S.M.A. Jubouri, S.M. Holmes, Hierarchical porous structured zeolite composite for removal of ionic contaminants from waste streams, Chim. Oggi Chem. Today, 35 (2017) 26–29.

[31] V.H. Montoya, M.A.P. Cruz, D.I.M. Castillo, M.R.M. Virgen, Competitive adsorption of dyes and heavy metals on zeolitic structures, J. Environ. Manage., 116 (2013) 213–221.

[32] S.M.A. Jubouri, N.A. Curry, S.M. Holmes, Hierarchical porous structured zeolite composite for removal of ionic contaminants from waste streams and effective encapsulation of hazardous waste, J. Hazard. Mater., 320 (2016) 241–251.

[33] L.R. Rad, A. Momeni, B.F. Ghazani, M. Irani, M. Mahmoudi, B. Noghreh, Removal of Ni²⁺ and Cd²⁺ ions from aqueous solutions using electrospun PVA/zeolite nanofibrous adsorbent, Chem. Eng. J., 256 (2014) 119–127.

[34] A.A.A. Rahmani, S.K.A. Attafi, S.K.A. Nasri, Z.W. Jasim, Hierarchical structures incorporating carbon and zeolite to remove radioactive contamination, Iraqi J. Sci., 61 (2020) 1944–1951.

[35] S.M.A. Jubouri, The static aging effect on the seedless synthesis of different ranges Faujasite-type zeolite Y at various factors, Iraqi J. Chem. Pet. Eng., 20 (2019) 7–13.

[36] M.N. Abbas, F.S. Abbas, H.H. Nussrat, S.N. Hussein, Synthesis of promoted catalyst from Iraqi rice husk used as a raw material for treating tannery wastewater, Aust. J. Basic Appl. Sci., 7 (2013) 511–528.

[37] R. Abid, G. Delahay, H. Tounsi, Preparation of LTA, HS and FAU/EMT intergrowth zeolites from aluminum scraps and industrial metasilicate, J. Mater. Cycles Waste Manage., 21 (2019) 1188–1196.

[38] L.M.G. Rodríguez, N.A.P. Durán, M.L. Cancino, G.A.F. Escamilla, D.A.D.H.D. Río, Synthesis of zeolite LTA using an agroindustrial residue as the SiO₂ precursor and evaluating its effectiveness in the removal of copper ions from water, Desal. Water Treat., 144 (2019) 156–165.

[39] A. Iqbal, H. Sattar, R. Haider, S. Munir, Synthesis and characterization of pure phase zeolite 4A from coal fly ash, J. Cleaner Prod., (2019) 258–267.

[40] S.M.A. Jubouri, Preparation of Highly-Reactive Silica from Phragmites (Common Reed) and Using It as an Inexpensive Silica Source to Prepare Y Zeolite, Patent 6291, 2020.

[41] S.M.A. Jubouri, S.I.A. Batty, S.M. Holmes, Using the ash of common water reeds as a silica source for producing high purity ZSM-5 zeolite microspheres, Microporous Mesoporous Mater., 316 (2021) 110953, doi: 10.1016/j.micromeso.2021.110953.

[42] H.S. Sherry, The ion-exchange properties of zeolites. I. Univalent ion-exchange in synthetic faujasite, J. Phys. Chem., 70 (1966) 1158–1168.

[43] A. Maes, A. Cremers, Ion exchange of synthetic zeolite X and Y with Co²⁺, Ni²⁺, Cu²⁺ and Zn²⁺ ions, J. Chem. Soc., Faraday Trans. 1 F, 71 (1975) 265–277.

[44] C.N. Mulligan, R.N. Yong, B.F. Gibbs, An evaluation of technologies for the heavy metal remediation of dredged sediments, J. Hazard. Mater., 85 (2001) 145–163.

[45] M.J. Harbottle, A.A. Tabbaa, C.W. Evans, A comparison of the technical sustainability of *in situ* stabilisation/solidification with disposal to landfill, J. Hazard. Mater., 141 (2007) 430–440.

[46] B.C. McLellan, R.P. Williams, J. Lay, A.V. Riessen, G.D. Corder, Costs and carbon emissions for geopolymer pastes in comparison to ordinary portland cement, J. Cleaner Prod., 19 (2011) 1080–1090.

[47] C. Shi, R. Spence, Designing of cement-based formula for solidification/stabilization of hazardous, radioactive, and mixed wastes, Crit. Rev. Environ. Sci. Technol., 34 (2004) 391–417.

[48] S.M.A. Jubouri, Synthesis of hierarchically porous ZSM-5 zeolite by self-assembly induced by aging in the absence of seeding-assistance, Microporous Mesoporous Mater., 303 (2020) 110296, doi: 10.1016/j.micromeso.2020.110296.

[49] S.M.A. Jubouri, D.A.D.H.D. Rio, A. Alfutimie, N.A. Curry, S.M. Holmes, Understanding the seeding mechanism of hierarchically porous zeolite/carbon composites, Microporous Mesoporous Mater., 268 (2018) 109–116.

[50] S.M.A. Jubouri, B.I. Waisi, S.M. Holmes, Rietveld texture refinement analysis of linde type A zeolite from X-ray diffraction data, J. Eng. Sci. Technol., 13 (2018) 4066–4077.

[51] M.H. Alhassani, S.M.A. jubouri, H.A.A. Jendeel, Stabilization of phenol trapped by agricultural waste: a study of the influence of ambient temperature on the adsorbed phenol, Desal. Water Treat., 187 (2020) 266–276.

[52] A. Nouri, M. Jafari, M. Kazemimoghadam, T. Mohammadi, Effects of hydrothermal parameters on the synthesis of nanocrystalline zeolite NaY, Clays Clay Miner., 60 (2012) 610–615.

[53] X. Zhang, D. Tang, M. Zhang, R. Yang, Synthesis of NaX zeolite: Influence of crystallization time, temperature and batch molar ratio SiO_2/Al_2O_3 on the particulate properties of zeolite crystals, Powder Technol., 235 (2013) 322–328.

[54] Z. Hajizadeh, K. Valadi, R.T. Ledari, A. Maleki, Convenient Cr(VI) removal from aqueous samples: executed by a promising clay-based catalytic system, magnetized by Fe_3O_4 nanoparticles and functionalized with humic acid, ChemistrySelect, 5 (2020) 2441–2448.

[55] S. Ahmed, S. Chughtai, M.A. Keane, The removal of cadmium and lead from aqueous solution by ion exchange with NaY zeolite, Sep. Purif. Technol., 13 (1998) 57–64.

[56] M.I. Ahamed, A.M. Asiri, Applications of Ion Exchange Materials in the Environment, Springer International Publishing, Switzerland, 2019.

[57] R. Nightingale, Phenomenological theory of ion solvation. Effective radii of hydrated ions, J. Phys. Chem., 63 (1959) 1381–1387.

[58] Database of Ionic Radii. Available at: http://Abulafia.Mt.Ic. Ac.Uk/Shannon/Radius.Php?Element=Hg

[59] R.D. Shannon, Revised effective ionic radii and systematic studies of interatomic distances in halides and chalcogenides, Acta Crystallogr., Sect. A Cryst. Phys. Diffr. Theor. Gen. Crystallogr., 32 (1976) 751–767.

[60] G. Sharma, D. Pathania, M. Naushad, N.C. Kothiyal, Fabrication, characterization and antimicrobial activity of polyaniline Th(IV) tungstomolybdophosphate nanocomposite material: efficient removal of toxic metal ions from water, Chem. Eng. J., 251 (2014) 413–421.

[61] S. Khandaker, Y. Toyohara, G.C. Saha, M.R. Awual, T. Kuba, Development of synthetic zeolites from bio-slag for cesium adsorption: kinetic, isotherm and thermodynamic studies, J. Water Process Eng., 33 (2020) 101055, doi: 10.1016/j. jwpe.2019.101055.

[62] D. Nibou, H. Mekatel, S. Amokrane, M. Barkat, M. Trari, Adsorption of Zn^{2+} ions onto NaA and NaX zeolites: kinetic, equilibrium and thermodynamic studies, J. Hazard. Mater., 173 (2010) 637–646.

[63] S. Bai, M. Chu, L. Zhou, Z. Chang, C. Zhang, B. Liu, Removal of heavy metals from aqueous solutions by X-type zeolite prepared from combination of oil shale ash and coal fly ash, Energy Sources Part A, (2019) 1–11, doi: 10.1080/15567036.2019.1661549.